ELSEVIER

Ceramics International 27 (2001) 261–264

CERAMICS INTERNATIONAL

www.elsevier.com/locate/ceramint

# Densification and grain growth during interface reaction controlled sintering of alumina ceramics

Zeming He *, Jan Ma

*School of Materials Engineering, Nanyang Technological University, Singapore 639798*

Received 18 January 2000; received in revised form 23 March 2000; accepted 24 May 2000

**Abstract**

This paper investigates the evolution of densification and grain growth during free sintering of pure alumina ceramics. In earlier work, interface reaction process was verified the dominant sintering mechanism of stage 1 of sintering of the material prepared here. We also limit our attention to stage 1 of sintering, i.e. when the porosity is in the form of interconnected channels. Based on the experimental data obtained and the constitutive laws employed, activation energies of densification and grain growth are determined. Grain size-relative density plot is plotted to express the development of densification and grain growth. 

*Keywords:* A. Grain growth; B. Interfaces; D. Alumina; Densification; Constitutive law

## 1. Introduction

Sintering is one of the most important processes for the production of ceramic materials. Almost all the ceramic materials have been made through the powder route, and also a variety of components used in modern technology have undergone sintering as one of the production steps. This may be one of the reasons why, compared to the economic importance and technical problems, publications on sintering studies are without doubt over-presented. Another reason is certainly the complexity of the sintering process that makes this field a fascinating area for research.

During the sintering of a powder compact, both densification and grain growth occur simultaneously [1]. It has been recognised that the relationship between densification and grain growth must be assessed in order to understand and control the sintering process. This requires a full understanding of the material constitutive laws governing the sintering process. The development of the constitutive relationship is closely related to the microstructural evolution of the sintering component. Several mechanisms are involved in the densification of a sintering powder compact [2]. For high temperature sintering of fine-grained materials, it is well accepted that diffusional mechanisms dominate the sintering process. It is also noted that the dominant path for diffusion is usually along the grain boundary [3]. Grain-boundary diffusion controlled sintering assumes that grain boundaries act as perfect sources and sinks for the diffusing atoms during the diffusion process. In practice, however, it is noted that some energy is expended in adding or removing a vacancy from a grain boundary, i.e. an interface reaction takes place. Therefore, the rate of densification can then be either controlled by the rate of diffusional transport between the sources and sinks or the rate at which the sources and sinks can provide, or accept, material for the diffusional process. The rate of operation of the sources and sinks is considered as interface reaction controlled sintering [4]. In diffusion processes, grain-boundary diffusion and interface reaction are two sequential processes, hence, the slower mechanism will dominate the sintering process. The smaller the mean grain size is, the shorter the transportation path is and therefore the faster the grain-boundary diffusion does, therefore, interface reaction become important. Ma [5] verified that the sintering mechanism of pure alumina ceramics is interface reaction dominant when grain size is less than 3 μm and indicated that the constitutive model of interface reaction proposed by Cocks [6] accurately describes the sintering process.

In the present work, pure alumina ceramics is prepared by powder route and some important parameters of sintering are evaluated. We limit our attention to stage 1 of sintering, i.e., when the porosity is in the form

* Corresponding author. Tel.: +65-790-4590; fax: +65-790-9081.
*E-mail address:* zmhe@ntu.edu.sg (Z. He).

0272-8842/01/$20.00 
PII: S0272-8842(00)00073-0

of interconnected channels [2,7], because the dominant densification mechanism of this stage was identified as interface reaction in earlier work [8]. Activation energies of densification and grain growth are determined by the constitutive law describing interface reaction proposed by Cocks [6] and grain-growth law proposed by Du and Cocks [9]. Grain size-relative density plot is drawn to express the trends of densification and grain growth during sintering.

## 2. Experimental procedure

The raw material for the experiment was Baikowski 99.99% ultrapure α-alumina powder with initial grain size 0.9 μm.

The raw powder was weighed and then it was fed into a steel die for compression. After being formed, the green compacts were placed in Carbolite RHF 1600 high-temperature electrical furnace for free sintering. The sintering profile was started with the heating rate of 2°C/min up to 600°C, and then with 10°C/min until the holding sintering temperature. The sintering temperatures chosen in this experiment were 1400, 1450, and 1500°C, respectively. For a given sintering temperature, different holding times were selected. They were 1, 3, 5, 10 and 15 h. The sample was cooled with the rate of 20°C/min to room temperature.

After the sample was prepared, mass was weighed by Scientech SA 510 analytical balance, and diameter and thickness were measured by Vernier calliper and Digital micrometer, respectively. The relative density, $\rho$, volumetric strain, $\varepsilon_v$, could be calculated from the measured data. This paper considers the value of volumetric strain positive, which is convenient for further determination.

JSM-5310 scanning microscope was employed to obtain the SEM image of the sample. The mean grain size measurement was determined by counting the number of grains traversed by a straight line of known length in the image. The final mean grain size, $L$, was taken as 1.56 times the average intercept length [10].

Other parameters, including volumetric strain rate, $\dot{\varepsilon}_v$, and grain-growth rate, $\dot{L}$, can be evaluated from the derivatives of the curves, which were plotted from the corresponding parameters, volumetric strain and grain size, against holding time, $t$.

Table 1
Experimental data of samples at sintering temperature of 1400°C

| $t$ (h) | $\rho$ | $L$ (μm) | $\varepsilon_v$ | $\dot{L}$ (μm/h) | $\dot{\varepsilon}_v$ (1/h) |
|---|---|---|---|---|---|
| 1 | 0.6364 | 1.026 | 0.221 | 0.1585 | 0.0567 |
| 3 | 0.6963 | 1.086 | 0.302 | 0.0634 | 0.0249 |
| 5 | 0.7271 | 1.114 | 0.340 | 0.0414 | 0.0170 |
| 10 | 0.7754 | 1.404 | 0.400 | 0.0233 | 0.0101 |
| 15 | 0.8111 | 1.623 | 0.439 | 0.0166 | 0.0075 |

## 3. Results and discussion

### 3.1. Sintering stages

The experimental results of the property parameters of the samples prepared at different sintering temperature and different holding time are shown in Tables 1–3. Once again, stage 1 of sintering is concentrated, and this classification was proposed by Ashby and co-workers [2,7], who divided the process of sintering into two stages based on the microstructure. The first stage, or stage 1, describes the early stage of densification when the pores are connected and discrete necks exist between the particles. The relative density of this stage is less than 0.9. For relative densities greater than 0.9, the pores close leaving isolated near equilibrium shaped pores between the grains. The material has then entered stage 2.

Fig. 1 shows one of the SEM images of the samples, which can be considered as the representative of the

Table 2
Experimental data of samples at sintering temperature of 1450°C

| $t$ (h) | $\rho$ | $L$ (μm) | $\varepsilon_v$ | $\dot{L}$ (μm/h) | $\dot{\varepsilon}_v$ (1/h) |
|---|---|---|---|---|---|
| 1 | 0.6965 | 1.193 | 0.303 | 0.3206 | 0.0757 |
| 3 | 0.8076 | 1.560 | 0.430 | 0.1445 | 0.0252 |
| 5 | 0.8512 | 1.805 | 0.478 | 0.0998 | 0.0151 |
| 10 | 0.8734 | 2.006 | 0.497 | 0.0604 | 0.0076 |
| 15 | 0.8864 | 2.674 | 0.509 | 0.0450 | 0.0050 |

Table 3
Experimental data of samples at sintering temperature of 1500°C

| $t$ (h) | $\rho$ | $L$ (μm) | $\varepsilon_v$ | $\dot{L}$(μm/h) | $\dot{\varepsilon}_v$ (1/h) |
|---|---|---|---|---|---|
| 1 | 0.8004 | 1.537 | 0.425 | 0.4533 | 0.0437 |
| 3 | 0.8735 | 2.028 | 0.495 | 0.2119 | 0.0163 |
| 5 | 0.8825 | 2.229 | 0.509 | 0.1488 | 0.0103 |
| 10 | 0.9267 | 3.008 | 0.549 | 0.0920 | 0.0055 |
| 15 | 0.9393 | 3.566 | 0.559 | 0.0696 | 0.0038 |

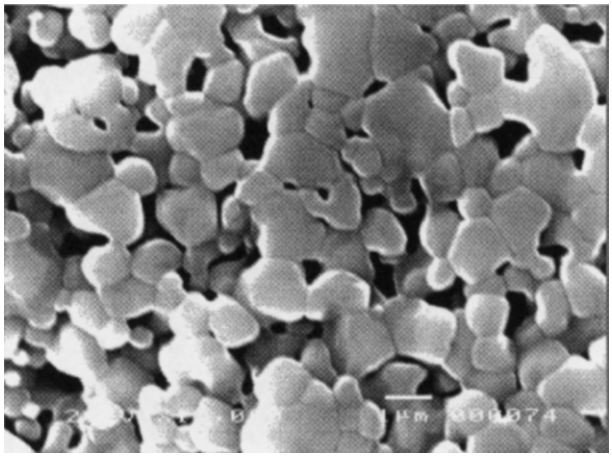

Fig. 1. SEM image of sintered sample (1500°C, 1h).

other samples, whose relative densities are less than 0.9, to be applied to reveal the microstructure. It is can be observed from Fig. 1, the microstructure shows loosely packed particles and pores form an interconnected network through the material.

### 3.2. Activation energies of sintering

In this subsection, the activation energies of densification and grain growth are evaluated by means of the constitutive laws of densification and gain growth.

When interface reaction is dominant, the volumetric strain rate for stage 1 can be obtained from Cocks [6] as

$$\dot{\varepsilon}_v = 3\dot{\varepsilon}_0\left(\frac{L_0}{L}\right)f(\rho)\left[c(\rho)\left(\frac{\sigma_e}{\sigma_0}\right)^{\frac{3}{2}}+f(\rho)\times\left(\frac{|3(\sigma_m-\sigma_s)|}{\sigma_0}\right)^{\frac{3}{2}}\right]\sqrt{\frac{\sigma_0}{|3(\sigma_m-\sigma_s)|}}\left[\frac{3(\sigma_m-\sigma_s)}{\sigma_0}\right] \quad (1)$$

where $\dot{\varepsilon}_0$ is the uniaxial strain rate under an applied stress $\sigma_0$ for a fully dense material of grain size $L_0$. $f(\rho)$ and $c(\rho)$ are dimensionless functions of the relative density, and $\sigma_e$, $\sigma_m$ and $\sigma_s$ are effective stress, mean stress and sintering potential, respectively. Sintering potential, or sintering stress, $\sigma_s$, is a fundamental parameter in the constitutive relationship. A porous compact will shrink during sintering, even without an externally applied load. This is due to the effect of sintering potential. For free sintering, in Eq. (1), $\sigma_m$ and $\sigma_e$ are all zero. The volumetric strain rate of free sintering then can be obtained as

$$\dot{\varepsilon}_v = 27\dot{\varepsilon}_0\left(\frac{L_0}{L}\right)f(\rho)^2\left(\frac{\sigma_s}{\sigma_0}\right)^2 \quad (2)$$

Compared with the mechanism of densification, grain-growth mechanism seems very simple, but it is also important for studying the sintering process. The driving force for this process is the difference in energy between fine-grained and large-grain particles resulting from the decrease in grain boundary and the total boundary energy. According to the grain-growth law presented by Du and Cocks [9], in stage 1, the equation for the grain-growth rate is

$$\dot{L} = \dot{L}_0\left(\frac{L_i}{L}\right)^3(1-\rho)^{-\frac{3}{2}} \quad (3)$$

where $\dot{L}_0$ is a temperature-dependent kinetic constant and $L_i$ is the initial grain size.

The activation energies of densification, $Q_d$, and grain growth, $Q_g$, have the relationship with $\dot{\varepsilon}_0$ and $\dot{L}_0$ as

$$\dot{\varepsilon}_0 = \dot{\varepsilon}_{00}\exp\left(\frac{-Q_d}{RT}\right) \quad (4)$$

and

$$\dot{L}_0 = \dot{L}_{00}\exp\left(\frac{-Q_g}{RT}\right) \quad (5)$$

where $\dot{\varepsilon}_{00}$ and $\dot{L}_{00}$ are material constants of densification and grain growth, which are independent of temperature. $R$ and $T$ are gas constant and absolute temperature, respectively.

By combining all the constants into one constant for the equation concerned, the volumetric strain rate [from Eq. (2)] and grain-growth rate [from Eq. (3)] can be derived as general forms at a given temperature as

$$\dot{\varepsilon}_v = df(\rho)^2\sigma_s^2\frac{1}{L} \quad (6)$$

and

$$\dot{L} = g(1-\rho)^{-\frac{3}{2}}\frac{1}{L^3} \quad (7)$$

respectively, $d$ and $g$ are combined constants of densification and grain growth respectively, they are still temperature-dependent. For a given sintering temperature, by fitting the experimental results of the volumetric strain rate, grain-growth rate, relative density and grain size, obtained at different holding time, to the corresponding Eqs. (6) and (7), the temperature-dependent constants, $d$ and $g$, at different sintering temperatures can be determined. The activation energies of densification and grain growth can then be evaluated by determining the slope of the curves of the logarithm of the corresponding temperature-dependent constants, $d$ and $g$, against the reciprocal of the absolute sintering temperature, $T$, see Fig. 2. During determination, the sintering potential and the dimensionless density function used are given by Ashby [2] and Du and Cocks [9] as

$$\sigma_s = \frac{6\gamma}{L}\rho^2\frac{2\rho-\rho_0}{1-\rho_0} \quad (8)$$

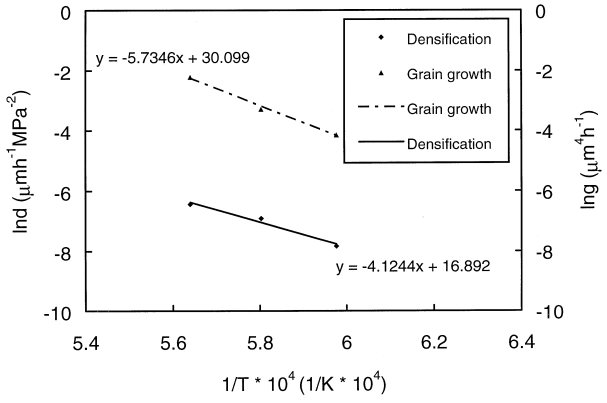


Fig. 2. Variation of logarithm of temperature-dependent constants with reciprocal of absolute sintering temperature.

and

$$f(\rho) = \frac{1}{3}\frac{(1-\rho_0)}{\rho^{\frac{3}{2}}\rho_0^{\frac{1}{2}}(\rho-\rho_0)} \tag{9}$$

respectively, where $\gamma$ is the surface energy per unit area of the materials (1 J/m$^2$ for alumina), and $\rho_0$ is the green relative density of the compact, which is taken as 0.5083. The value of initial grain size, $L_i$, is taken as 0.9 μm for calculation.

The densification activation energy and grain-growth activation energy, determined from Fig. 2, are 342 KJ/mol and 476 KJ/mol, respectively. The value of densification activation energy is close to the one determined by Ma [5], 325 KJ/mol, when interface reaction is the dominant sintering mechanism. This value indicates again that interface reaction is the controlled process of the material under investigated.

By comparing the activation energies, it can be found that the value of grain-growth activation energy is larger than the value of densification activation energy. This result provides a thermodynamic prediction for the evolution relationship between densification and grain growth in stage 1. The behavior of densification proceeds more easily compared with the process of grain growth, due to higher grain-growth activation energy.

### 3.3. Grain size-relative density plot

The grain size-relative density plot of the sintered samples in stage 1, at different sintering temperature, is generated to express the relationship of densification and grain growth, which is shown in Fig. 3. In such a plot, the path along which the state of the material evolves can be known.

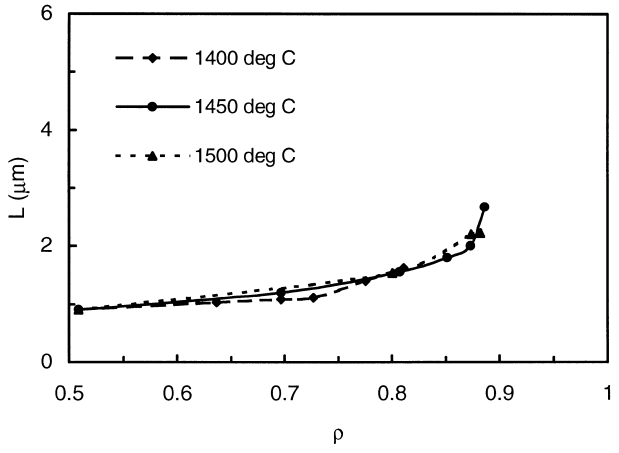


Fig. 3. Grain size-relative density plot.

It can be seen from Fig. 3 that grain size increases with increasing density. In stage 1, the increasing rate of the grain size (from 0.9 to 2.674 μm) changes very slowly as the change of the relative density (from 0.5083 to 0.8864). This behavior is in conformity with the thermodynamic prediction presented in Subsection 3.2. The feature of the microstructure in stage 1 can be used to explain this phenomenon. Actually, the slower grain growth in stage 1 is caused by the interconnected pores, which have a strong pinning effect on the grain boundary and restrain grain-boundary movement.

## 4. Conclusions

This paper investigates the evolution of densification and grain growth during stage 1 of sintering of pure alumina ceramics, when interface reaction process is the dominant sintering mechanism. Densification activation energy and grain-growth activation energy are determined as 342 and 476 KJ/mol, respectively, by means of the constitutive laws employed and experimental parameters achieved. From the results of activation energies of densification and grain growth determined, and grain size–relative density plotted, it is concluded that grain grows very slowly compared with densification in stage 1 of sintering, due to the pinning effect of the interconnected pores on grain-boundary movement.

## References

[1] N.J. Shaw, Densification and coarsening during solid state sintering of ceramics: a review of the models — III. Coarsening, Powder, Metall. Int. 21 (5) (1989) 25–29.
[2] M.F. Ashby, Background Reading HIP 6.0, Technical report, University of Cambridge, 1990.
[3] W.D. Kingery, H.K. Bowen, D.R. Uhlmann, Introduction to Ceramics, John Wiley & Sons, USA, 1960.
[4] J. Pan, A.C.F. Cocks, A constitutive model for stage 2 sintering of fine grained materials — II Effects of an interface reaction, Acta Metall. Mater. 42 (4) (1994) 1223–1230.
[5] J. Ma, Constitutive modeling of the densification of porous ceramic components, PhD thesis, University of Cambridge, 1997.
[6] A.C.F. Cocks, The structure of constitutive laws for the sintering of fine grained materials, Acta Metall. Mater. 42 (7) (1994) 2191–2210.
[7] A.S. Helle, K.E. Easterling, M.F. Ashby, Hot isostatic pressing diagrams: new developments, Acta Metall. 33 (12) (1985) 2163–2174.
[8] J. Ma, Z. He, M.J. Tan, Constitutive modeling of sintering of alumina ceramics, in: Proceedings of the 8th International Conference on Processing and Fabrication of Advanced Materials, 8–10 September 1999, Singapore.
[9] Z.Z. Du, A.C.F. Cocks, Sintering of fine-grained materials by interface reaction controlled grain-boundary diffusion, Int. J. Solids Struct. 31 (10) (1994) 1429–1445.
[10] M. Rahaman, L. De Jonghe, R.J. Brook, Effect of shear stress on sintering, J. Am. Ceram. Soc. 69 (1) (1986) 53–58.